Asian Journal of Chemistry; Vol. 37, No. 12 (2025), 3079-3085
ASIAN JOURNAL OF CHEMISTRY
https://doi.org/10.14233/ajchem.2025.34733

Eco-Engineered Copper Oxide Nanoparticles *via* Microwave-Assisted Extraction of *Cyphostemma auriculatum* (Roxb.): Synthesis, Characterization and Bioactivity Evaluation

ASHLESHA ARUN WAKCHAURE[1,*], MANOJ RAMESH KUMBHARE[1] and SONALI RAMRAO GAWALI[2]

[1]Department of Pharmaceutical Chemistry, S.M.B.T. College of Pharmacy (Affiliated to Savitribai Phule Pune University), Nashik-422403, India
[2]Department of Pharmacognosy, M.V.P. Samaj's College of Pharmacy, (Affiliated to Savitribai Phule Pune University), Nashik-422002, India

*Corresponding author: E-mail: wakchaureashlesha01@gmail.com

Received: 20 August 2025 *Accepted*: 15 October 2025 *Published online*: 30 November 2025 AJC-22198

As nanotechnology continues to expand the therapeutic applications of metal oxide nanoparticles across diverse diseases, this study emphasized on the green synthesis of copper oxide nanoparticles (CuO NPs) using ethanolic extract of *Cyphostemma auriculatum* (Roxb.). This eco-friendly synthesis yielded CuO NPs with reduced particle size and enhanced stability while eliminating the use of hazardous chemicals. Employing the ethanolic extract of *C. auriculatum* (Roxb.), the study synthesized CuO NPs and subsequently evaluated their antimicrobial activity. The synthesized CuO NPs were characterized using UV-visible spectrophotometry, zeta potential analysis, FTIR spectroscopy, transmission electron microscopy (TEM), particle size analysis, scanning electron microscopy (SEM) and X-ray diffraction (XRD) to assess their structural, morphological and functional properties. UV-Vis spectroscopy displayed a distinct absorption peak at 532 nm, confirming the successful formation of CuO NPs. FTIR analysis identified phenolic compounds whose carbonyl and hydroxyl groups facilitated copper ion reduction and nanoparticle stabilization. The synthesized CuO NPs exhibited an average hydrodynamic size of 122 nm with a PDI of 0.389, indicating moderate dispersion. SEM revealed predominantly spherical particles, while TEM further showed a uniform size distribution within the 2-10 nm range, validating their nanoscale morphology. Moreover, the antimicrobial activity and *in vitro* and *in vivo* anti-inflammatory of the synthesized CuO NPs was further investigated. The results demonstrate that plant extracts can effectively tailor the properties of CuO NPs, thereby enhancing their functional performance. Among the tested extracts, the ethanolic extract *of C. auriculatum* (Roxb.) produced CuO nanoparticles with the highest antimicrobial activity. This green synthesis approach not only improves nanoparticle efficacy but also provides an eco-friendly and cost-effective route for nanoparticle production.

Keywords: Copper oxide nanoparticles, *C. auriculatum* (Roxb.), Polydispersity index, Antimicrobial activity, Anti-inflammatory.

INTRODUCTION

The demand for metallic nanoparticles has increased substantially due to their unique physico-chemical properties, including surface plasmon resonance (SPR) and significant biological, optical and electrical characteristics [1], leading to growing interest among scientists and researchers worldwide [2]. Green chemistry and green nanotechnology, collectively known as green synthesis approaches, employ environmentally benign precursor materials and solvents to produce nanomaterials while aiming to minimize or eliminate hazardous byproducts in the reaction medium. Common metals used in green nanoparticle synthesis include aluminium, gold, silver, platinum, copper, lead, zinc, nickel and iron [3]. Among these, copper oxide (CuO) nanoparticles have gained significant attention due to their diverse applications as catalysts, superconductors, dye degradation agents and fungicides, as well as their strong antibacterial and potential anticancer activities, making them valuable in semiconductor, cosmetic and medical industries [4]. Given their extensive biomedical relevance, the use of non-toxic solvents, stabilizers and reducing agents in CuNPs synthesis is essential, underscoring the importance of biosynthetic, bottom-up approaches for producing safe and sustainable nanoparticles [5].

Cyphostemma species are known for their antimalarial, anticancer, antitumor and antihelminthic properties and have long been used in Ethiopia to treat ailments like rabies, snake bites and skull injuries [6]. Several bioactive compounds found

in *C. auriculatum* (Roxb.), a member of the Vitaceae family, add to its therapeutic efficacy. Numerous chemical compounds with various kinds of pharmacological and biological properties are present in this plant [7,8].

According to literature survey, no previous studies on the integration of microwave-assisted extraction (MAE) and nanoparticle synthesis using this plant species. So, green synthesis of CuO NPs by employing *C. auriculatum* (Roxb.) plant with ethanolic extract and furthermore, the comparative biological evaluation (especially both antimicrobial and *in vitro* anti-inflammatory activities) of the synthesized CuO NPs *versus* crude extract is also not well-documented.

The primary objective of the present study was to employ microwave-assisted extraction (MAE) for the efficient recovery of phytoconstituents from *C. auriculatum* (Roxb.), followed by the synthesis and characterization of CuO NPs using the plant extract. The secondary objective was to evaluate the antimicrobial activity of the plant extract against multidrug-resistant bacterial strains and to assess the *in vitro* anti-inflammatory activity of both the biosynthesized CuO NPs and the crude plant extract. The results demonstrate that the CuO NPs exhibited enhanced biological activity compared to the crude extract, highlighting the efficacy and potential advantages of metallic nanoparticle-based formulations.

EXPERIMENTAL

All chemicals used were of analytical reagent (AR) grade and were utilized without further purification. Copper(II) sulphate pentahydrate and sodium hydroxide (98.5%, analytical grade) as well as ethanol (99.8%, analytical grade) were procured from Research Lab Fine Chem Industries, Mumbai, India. Deionized water was used throughout the experimental work.

Collection of plant: Fresh plant of *C. auriculatum* Roxb. was collected from area of Trimbakeshwar (19.9361º N, 73.5358º E), District Nashik, India. The plant material was collected during the flowering and fruiting season for proper botanical identification and recognized by Botanical Survey of India, Western Regional Centre, Pune, with certification no. BSI/WRC/Iden,Cer./2021/1111210001787.

Approval of IAEC committee: IAEC committee approval has been certified for Biotax Laboratories under project no. Biotox/IAEC/03/2024/RP-11 for animal studies.

Processing of the plant material: The whole plant was rinsed, approximately three-quarters was shade-dried and subsequently pulverized, while the remaining one-quarter was reserved for leaf separation.

Microwave-assisted extraction: A microwave oven operating at 280 W irradiation power was employed for conducting microwave assisted extraction (MAE) with 10 g of leaves. MAE was performed for 5 min at 50 ºC with ethanol as solvent. The irradiation cycle was performed in 60 sec intervals, with the solvent–sample mixture subjected to extraction for a total of 5 min. The resulting extract was cooled and filtered through Whatman filter paper for subsequent use [9].

Synthesis of CuO NPs: CuO NPs were synthesized in accordance with the reported method [10], with the following modification. In a homogeneous solution $CuSO_4 \cdot 5H_2O$ (0.1 M) solution, a magnetic stirrer was used to maintain the solution temperature on a hot plate. The green extract of *C. auriculatum* (Roxb.) was added dropwise using a burette while continuously stirring. The reaction was maintained at 60 ºC and pH 10 throughout the experiment. Stirring was continued after the solution colour changed, with pH adjusted as needed using 1 M NaOH. The reaction mixture was again stirred for an additional 2 h to ensure complete formation of nanoparticles, which settled at the bottom. The nanoparticles were collected by centrifugation at 4000 rpm for 15 min and washed three times with water and acetone. The purified nanoparticles were then dried in a hot-air oven at 60 ºC for 2 h, yielding a dark green powder, which was stored at room temperature for further use.

Characterization: UV–vis spectroscopy (Shimadzu) was employed to confirm nanoparticle formation through detection of characteristic surface plasmon resonance (SPR) peaks in the 190-800 nm range. Functional groups on the nanoparticle surface were identified using FTIR analysis with a Bruker Alpha spectrophotometer over 4000-400 cm^{-1}. Particle size and size distribution were determined *via* dynamic light scattering (DLS) using a Horiba SZ100, confirming stable and uniformly dispersed nanoparticles. Zeta potential measurements assessed the surface charge and suspension stability. Structural features and surface morphology were examined using scanning electron microscopy (SEM), revealing predominantly spherical particles with smooth surfaces, while transmission electron microscopy (TEM) provided high-resolution images to evaluate particle size, morphology and distribution. Crystalline structure, phase purity and average crystallite size were analyzed using X-ray diffraction (XRD) at a scanning rate of 0.4º/min over a 2θ range of 10-70º.

Antimicrobial activity: *In vitro* antimicrobial activity was assessed utilizing agar well diffusion method [11,12]. Sterile nutrient agar was inoculated with the bacterial cultures and incubated at 37 ºC for 48 h. Antimicrobial potential was tested against selected bacteria like *P. aeruginosa*, *S. aureus*, *B. subtilis* and *E. coli*. Bacterial inocula were prepared from actively growing cultures. Approximately 15 mL of nutrient agar (HiMedia) was poured into sterile Petri dishes and permitted to solidify. Each plate was then uniformly inoculated with 100 µL of bacterial broth utilizing sterile spreader. Once surface dried, wells of 6 mm diameter were made using sterile cork borer. Test compounds were dissolved in DMSO to a concentration of 1 mg/mL. Volumes of 100 µL of each test solution and standard were added to wells. Streptomycin (1 mg/mL) served as positive control, while DMSO alone was utilized as negative control. After incubation at 37 ºC for 24 h, the antimicrobial efficacy has been assessed by calculating diameter of zones of inhibition (ZI) around each well. All the experiments were conducted in triplicate for ensuring accuracy and reproducibility

Acute oral toxicity study: An acute oral toxicity study was conducted for both the plant extract and the green-synthesized CuO NPs following OECD guideline no. 423. The limit test was performed using healthy Swiss albino mice (20-25 g) with six animals in each group. A single administration of 2000 mg/kg body weight was performed. The plant extract was dissolved in distilled water and the CuO NPs were

suspended in 0.5% carboxymethyl cellulose (CMC) to ensure uniform dispersion.

After administration, the animals were closely monitored for signs of toxicity, behavioural changes and mortality during the first 48 h, followed by daily observations for a total period of 14 days. No signs of toxicity or mortality were observed in either group throughout the study, indicating that both the plant extract and CuO NPs were safe at the tested dose under the experimental conditions.

In vitro anti-inflammatory activity

Human red blood cell (HRBC) method: The human red blood cell (HRBC) membrane stabilization method has been useful for assessing *in vitro* anti-inflammatory activity of plant extracts and green synthesized CuO NPs. Fresh blood obtained from healthy human volunteer had refrained from consuming non-steroidal anti-inflammatory drugs (NSAIDs) for minimum 2 weeks. For avoiding clotting, collected blood was promptly combined with equivalent amount of Alsever's solution (0.5% citric acid, 0.8% sodium citrate, 0.42% NaCl and 2% dextrose) were diluted in distilled water. Red blood cells (RBCs) were separated from the blood-Alsever combination by centrifuging it for 20 min at 3000 rpm. RBCs were then rinsed three times with 0.36% hyposaline solution. Phosphate buffer (0.15 M, pH 7.4) was employed to generate 10% RBC suspension. A 1.1 mL of test extract and CuO NPs at varying concentrations was combined with 2 mL of hyposaline, 1 mL of phosphate buffer, 0.5 mL of 10% RBC suspension for assay. Reaction mixtures centrifuged at 3000 rpm for 20 min after being incubated at 37 ºC for 30 min. UV-Vis spectrophotometer was employed for measuring absorbance of resultant supernatant at 560 nm. The percentage protection (membrane stabilization) was calculated by using the following formula:

$$\text{Protection (\%)} = \frac{\text{OD of control}}{\text{OD of test}} \times 100$$

A control sample (without extract), absorbance of the control sample was found to be 0.242 and a standard drug sample (*e.g.* diclofenac sodium) were used for comparison [13,14].

***In vivo* carrageenan-induced paw edema:** The acute anti-inflammatory activity was assessed using the method as described by Winter *et al.* [15]. Experimental animals were randomly assigned into six groups, each consisting of six rats. Group I served as the negative control, receiving only the vehicle. Group II acted as the positive control, treated with the standard anti-inflammatory drug. Groups III, IV, (ethanolic extract 200 mg/kg and 400 mg/kg) and Groups V, VI (CuO NPs 200 µg/kg and 400 µg/kg), orally. After 1 h, all animals were injected with 0.1 mL of 1% carrageenan solution (prepared in 1% CMC) into the sub plantar region of the left hind paw to induce inflammation. The right hind paw was injected with 0.1 mL of vehicle to serve as an internal control. Diclofenac sodium (10 mg/kg) was used as the reference standard for comparison. Paw swelling was measured using a digital Vernier caliper at 0, 30 min, 1, 2, 3, 4 and 5 h following carrageenan injection [16,17].

The anti-inflammatory activity of each treatment group was determined by comparing their paw edema measurements with that of the control group. The percentage inhibition of inflammation was calculated using the following formula:

$$\text{Inhibition (\%)} = \frac{V_c - V_t}{V_c} \times 100$$

where V_c = mean paw thickness in the control group and V_t = mean paw thickness in the treated group.

RESULTS AND DISCUSSION

The initial confirmation of CuO NPs synthesis was indicated by a visible colour change. Upon treatment of aqueous copper sulphate ions with the plant ethanolic extract, reduction of the ions occurred, causing mixture to gradually change from light blue to light green to dark green, which confirmed the formation of CuO NPs.

UV-Vis spectral studies: The formation of CuO NPs was confirmed by recording their absorption spectra in the 200-800 nm range (Fig. 1). The UV-Vis spectrum of the synthesized CuO NPs exhibited a characteristic peak at 410 nm, corresponding to the surface plasmon resonance (SPR), indicating successful nanoparticle formation and uniform particle size distribution.

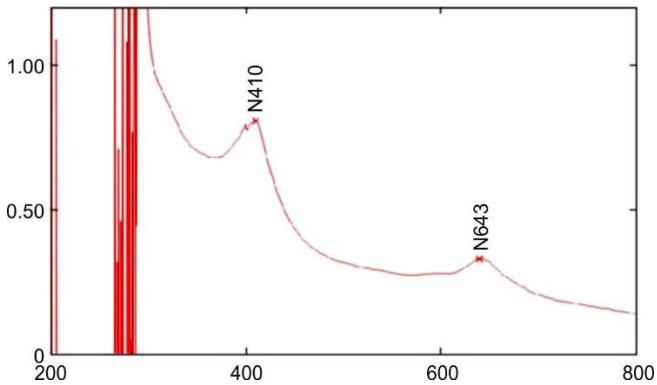

Fig. 1. Surface plasmon resonance exhibited by CuO NPs

FTIR spectral studies: The *C. auriculatum* (Roxb.) leaf extract and synthesized CuO NPs of extract have exhibited substantial modifications in their FTIR spectra. Alkyl halides band, particularly C-Cl bond, was primary concern of the FTIR spectrum of ethanolic extract (Fig. 2a), which exhibited a peak in 800-600 cm^{-1} range. Distinct peak observed at 874.19 cm^{-1} corresponds to out-of-plane vibrations of C–H bonds associated with alkenes and alkynes, which are commonly present in plant extracts. A distinct peak at 1014.89 cm^{-1} can be showed the C–OH group, typically arising from proteins present in the plant extract. Prominent peak at 1279.51 cm^{-1} is assigned to C–O stretching vibrations of ester, carboxylic acid and ether groups, which are commonly present in plant extracts. Sharp peak at 1720.21 cm^{-1} similar to C=O stretching vibrations of carbonyl groups, like those found in ketones, carboxylic acids or aldehydes. Absorption bands observed at 2970.78 cm^{-1} and 2924.78 cm^{-1} are ascribed to symmetric and asymmetric stretching vibrations of aliphatic C–H bonds, respectively. Broad absorption band at 3360.90 cm^{-1} has been assigned to

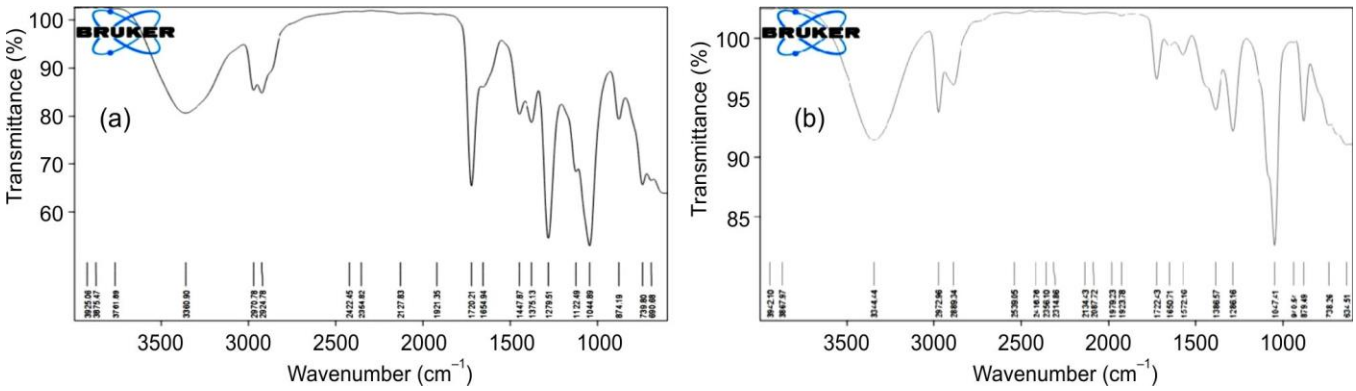

Fig. 2. FTIR spectra of (a) ethanolic extract of *C. auriculatum* Roxb. and (b) CuO NPs of ethanolic extract of *C. auriculatum* Roxb.

O–H stretching vibrations of hydroxyl groups, indicating presence of phenols, alcohols or carboxylic acids in the plant extract. The Cu-O bond vibrational frequencies led to a distinct peak observed at 634.51, 738.26, 879.49 and 940.54 cm^{-1} in synthesized CuO NPs of extract. In synthesized CuO NPs, bending absorptions were observed in 879.49 cm^{-1} due to the Cu–O–H bonding. The synthesis of CuO NPs in present investigation was found to be robust, as nanoparticles were able to be produced under a wide spectrum of conditions (Fig. 2b). Distinct peak at absorption band at 1047.41 cm^{-1} is attributed to C–OH stretching vibrations. A major peak at 1286.16 cm^{-1} C–O stretching vibrations typically associated with carboxylic acids, esters or phenolic compounds present in the plant extract. Sharp peak at 1386.57 cm^{-1} showed the C-OH stretching vibrations whereas another sharp peak at 1722.43 cm^{-1} corresponds to the C=O stretching vibrations of carbonyl groups. Distinct peak at 2889.34 cm^{-1} showed presence of alkanes while the absorption peak at 2972.96 cm^{-1} is attributed to the C-H asymmetric stretching in alkanes. The broad absorption band at 3344.44 cm^{-1} is assigned to the O–H stretching vibrations in alcoholic and phenolic compounds [18,19].

Particle size analysis: As illustrated in Fig. 3, the average particle size of the synthesized CuO NPs was approximately 95.4 nm, which falls within the expected nanoscale range. The particles exhibited a polydispersity index (PDI) of 0.311, indicating a relatively uniform and monodispersed distribution, which is favourable for consistent biological and catalytic performance.

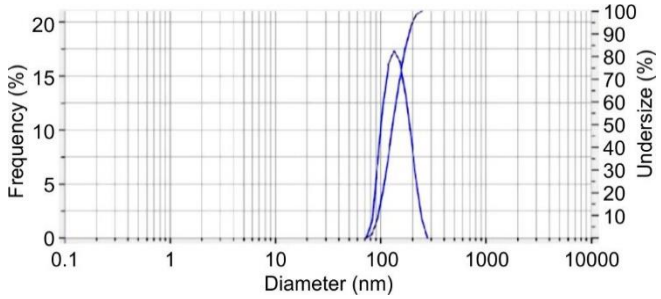

Fig. 3. Particle size and PI analysis of synthesized of CuO NPs of ethanolic extract of *C. auriculatum* Roxb.

Zeta potential: The colloidal stability of the synthesized CuO NPs was evaluated using zeta potential measurements. As shown in Fig. 4, the CuO NPs exhibited a zeta potential of –10.4 mV, indicating a moderate to high level of electrostatic stability in suspension.

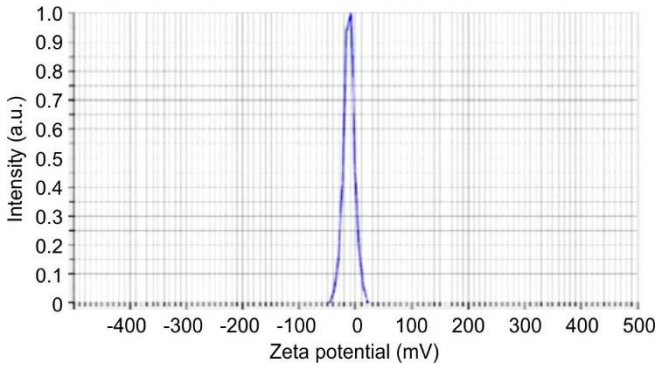

Fig. 4. Zeta potential analysis of synthesized of CuO NPs of ethanolic extract of *C. auriculatum* Roxb.

Morphological studies: SEM analysis of CuO NPs synthesized using the ethanolic extract of *C. auriculatum* (Roxb.) revealed predominantly spherical and circular particles with well-defined surface morphology and self-aligned prismatic arrangements, as shown in Fig. 5 [20,21]. TEM images further confirmed that the nanoparticles were mostly spherical with uniform size distribution, consistent with previous reports of copper nanoparticles synthesized *via* eco-friendly, plant-mediated methods (Fig. 6) [19].

XRD studies: The XRD spectrum of the synthesized CuO NPs revealed prominent peaks at 2θ values of 29.89º, 31.87º, 34.12º, 36.84º, 44.79º, 50.49º and 54.33º, corresponding to the crystallographic planes (101) (011), (200), (111), (202), (211) and (031), respectively (Fig. 7). The sharp and well-defined peaks indicate a highly crystalline structure with excellent nanoparticle distribution, confirming the successful formation of crystalline CuO nanoparticles [22-24].

Antimicrobial activity: Agar well diffusion method has been employed for evaluating antimicrobial potential of green-synthesized CuO nanoparticles against representative strains of Gram-positive (*B. subtilis* ATCC 11774, *S. aureus* ATCC 23235) and Gram-negative (*P. aeruginosa* ATCC 27853, *E. coli* ATCC 9637) bacteria. The antibacterial activity of the green synthesized CuO NPs and the ethanolic extract of *C. auriculatum* (Roxb.) was evaluated by measuring the diameter of inhibition zones (mm) around each well, as presented in Table-1. The CuO NPs exhibited significant antibacterial activity against all tested pathogens, with the maximum inhibi-

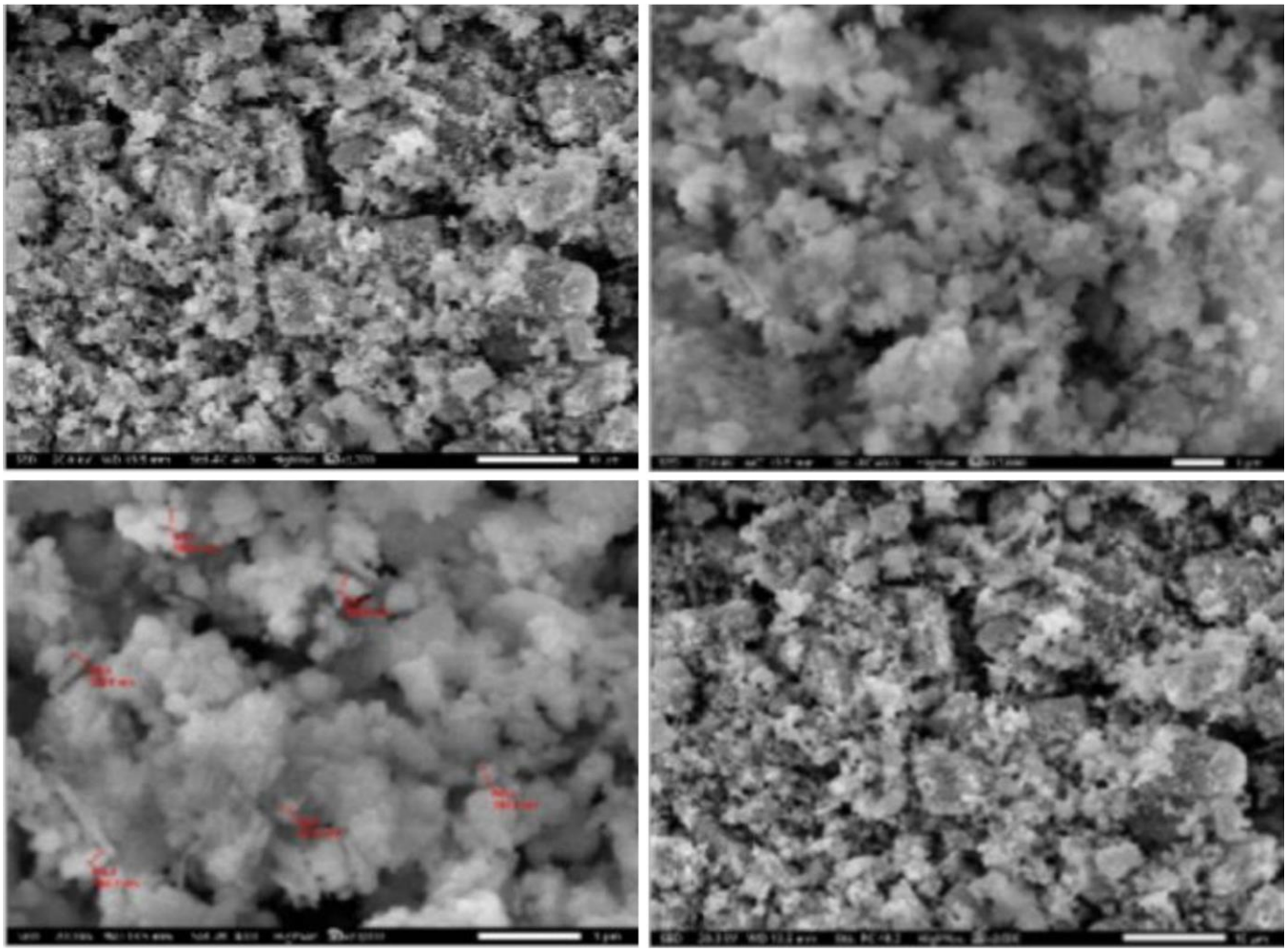

Fig. 5. SEM images of synthesis of CuO NPs from ethanolic extract of *C. auriculatum* Roxb. under high magnification energy

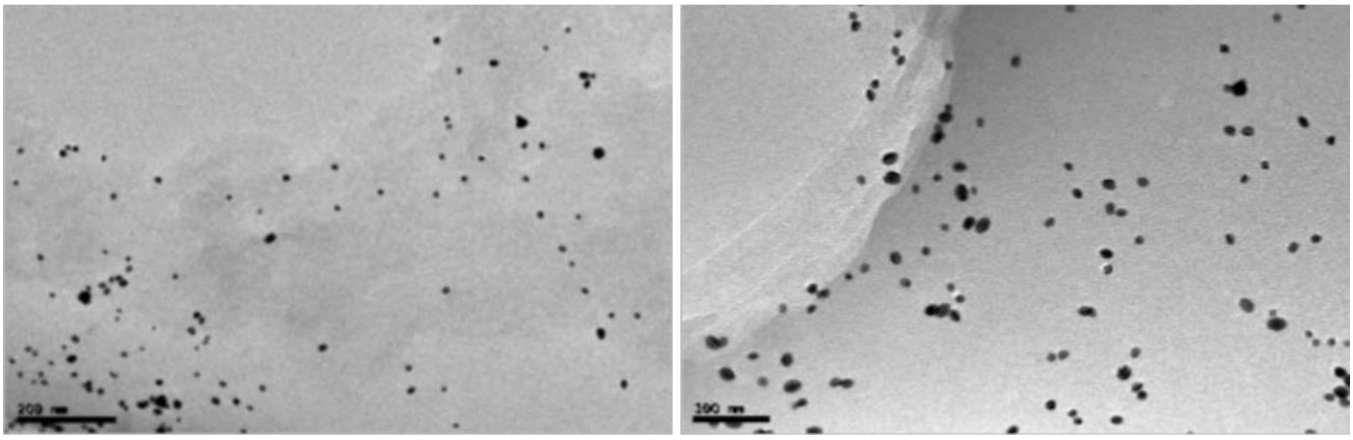

Fig. 6. TEM images of synthesized of CuO NPs of ethanolic extract of *C. auriculatum* Roxb. at 200 nm and 100 nm

TABLE-1
ANTIMICROBIAL ACTIVITY OF CuO NPs AGAINST DIFFERENT BACTERIAL STRAINS

Test of organism	Zone of inhibition (mm)			
	Control	Standard (streptomycin)	CA extract	CuO NPs
E. coli ATCC 9637	00	24	13	20
P. aeruginosa ATCC 27853	00	22	09	16
S. aureus ATCC 23235	00	25	14	21
B. subtilis ATCC 11774	00	28	12	16

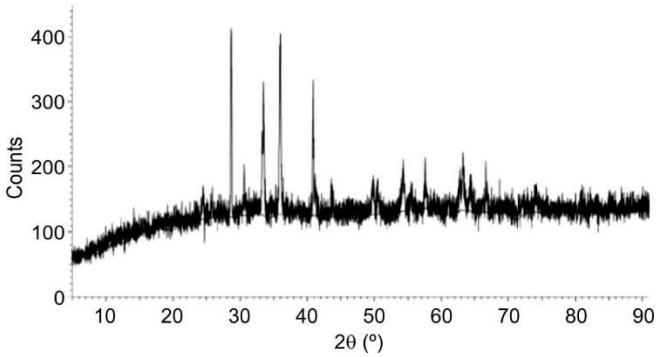

Fig. 7. XRD spectra of synthesized of CuO NPs of ethanolic extract of *C. auriculatum* Roxb.

tion observed against *S. aureus* (21 mm), followed by *E. coli* (20 mm). *P. aeruginosa* and *B. subtilis* displayed inhibition zones of 16 mm, indicating the relatively lower sensitivity. In comparison, the ethanolic plant extract showed moderate antibacterial activity, with the highest inhibition against *S. aureus* (14 mm), followed by *E. coli* (13 mm), *B. subtilis* (12 mm), and the least against *P. aeruginosa* (9 mm). Streptomycin was used as a positive control to validate the assay. Overall, the CuO NPs demonstrated superior antimicrobial efficacy compared to the crude plant extract, suggesting that green-synthesized CuO NPs may serve as potent antibacterial agents.

Acute oral toxicity study: No treatment-related mortality or clinical signs of toxicity were observed in the ethanolic extract and CuO NPs-treated group during the 14-day observation period. Body weight gain in treated animals was comparable to controls. Gross necropsy revealed no visible abnormalities. Based on these findings, the oral LD_{50} of the tested is greater than 2000 mg/kg under the experimental conditions used.

***In vitro* anti-inflammatory activity (HRBC method):** In this study, varying concentrations (100–1000 µg/mL) of plant extract and its synthesized CuO NPs were tested for their ability to stabilize the RBC membrane. A negative control group, consisting of Alsever's solution with blood in it instead of test sample, was used to represent 100% haemolysis (no protection). At 1000 µg/mL, diclofenac sodium showed a maximum membrane stabilization of 86.97%. Among the test samples, the CuO NPs exhibited the highest activity with 71.09% stabilization, while the plant extract showed 52.84% at the same concentration. The results suggest that both the extract and CuO NPs possess significant anti-inflammatory properties, with CuO NPs showing enhanced effectiveness, likely due to improved bioavailability or synergistic action. The detailed percentage membrane stabilization results for both samples are provided in Table-2.

TABLE-2
In vitro ANTI-INFLAMMATORY ACTIVITY OF ETHANOLIC EXTRACTS *C. auriculatum* Roxb. AND CuO NPs (HRBC METHOD)

Conc. (µg/mL)	Membrane stabilization (%)		
	Std.	Ethanolic extract	CuO NPs
100	38.83 ± 0.87***	13.45 ± 0.67***	21.82 ± 0.87***
200	43.06 ± 0.89***	21.57 ± 0.78***	33.92 ± 0.84***
400	52.21 ± 0.97***	32.48 ± 0.67***	42.37 ± 0.78***
600	64.89 ± 0.87***	40.58 ± 0.54***	54.86 ± 0.74***
800	71.84 ± 0.97***	48.97 ± 0.67***	63.32 ± 0.78***
1000	86.97 ± 0.78***	52.84 ± 0.58***	71.09 ± 0.67***

Values are shown as mean ± SEM, n = 3.

***In vivo* anti-inflammatory activity (Carrageenan induced paw edema model):** In this system, both the ethanolic extract and CuO NPs of *C. auriculatum* Roxb. significantly reduced carrageenan-induced paw edema in a dose-dependent manner. The extract showed moderate activity, with the high dose (400 mg/kg) producing. In contrast, CuO NPs were more potent, as even the low dose (200 µg/kg) significantly suppressed edema, while the high dose (200 µg/kg) achieved ($p < 0.001$) with standard drug, diclofenac (10 mg/kg) (Table-3). These results indicate that CuO NPs exhibit superior anti-inflammatory activity compared to the crude extract, approaching the efficacy of the standard drug.

Conclusion

The present study successfully demonstrates the green synthesis of copper nanoparticles (CuO NPs) using the ethan-

TABLE-3
In vivo ANTI-INFLAMMATORY ACTIVITY OF ETHANOL EXTRACTS *C. auriculatum* Roxb. AND CuO NPs (CARRAGEENAN-INDUCED PAW EDEMA MODEL)

Group	Treatment	Paw volume (mm)						
		0 min	30 min	1 h	2 h	3 h	4 h	5 h
Control	Without drug (vehicle)	4.15 ± 0.12***	6.25 ± 0.15***	7.12 ± 0.17***	8.34 ± 0.09***	9.21 ± 0.11***	9.45 ± 0.15***	9.35 ± 0.14***
Standard	Diclofenac (10 mg/kg) orally	4.62 ± 0.08***	5.24 ± 0.07***	5.47 ± 0.19***	5.54 ± 0.15***	5.21 ± 0.17***	4.75 ± 0.08***	4.27 ± 0.16***
Group I	Ethanolic extract (200 mg/kg)	4.72 ± 0.18***	5.51 ± 0.15***	6.12 ± 0.14***	6.38 ± 0.17***	6.14 ± 0.18***	5.34 ± 0.16***	4.94 ± 0.14***
Group II	Ethanolic extract (400 mg/kg)	4.86 ± 0.11***	5.34 ± 0.17***	5.97 ± 0.12***	6.04 ± 0.16***	5.75 ± 0.15***	5.04 ± 0.13***	4.75 ± 0.12***
Group III	CuO NPs (200 µg/kg)	4.67 ± 0.15***	5.02 ± 014***	5.75 ± 0.15***	5.91 ± 0.12***	5.68 ± 0.14***	4.97 ± 0.18***	4.57 ± 0.16***
Group IV	CuO NPs (400 µg/kg)	4.45 ± 0.14***	4.97 ± 0.04***	5.48 ± 0.18***	5.62 ± 0.09***	5.39 ± 0.16***	4.57 ± 0.12***	4.36 ± 0.08***

Values are shown as mean ± SEM, n = 6.

olic extract of *C. auriculatum* Roxb. through a simple, eco-friendly and efficient method. Microwave-assisted extraction played a crucial role in enhancing the phytochemical yield from the plant, which facilitated the reduction and stabilization of CuO NPs. Comprehensive characterization through UV-Vis, FTIR, XRD, TEM and SEM, confirmed the successful formation of stable, spherical and crystalline CuO NPs. The presence of bioactive compounds in the plant extract not only enabled nanoparticle synthesis but also enhanced their biological activities. The synthesized CuO NPs also exhibited remarkable antimicrobial activity against both Gram-positive and Gram-negative bacteria. Furthermore, the *in vitro* through RBC membrane stabilization and *in vivo* anti-inflammatory activity through carrageenan-induced paw edema model, revealed that CuO NPs provided significant membrane protection and suppress paw edema, surpassing the activity of the crude extract and showing results comparable to the standard drug. Overall, the study highlights the therapeutic potential of biosynthesized CuO NPs, suggesting their possible application in developing novel antimicrobial and anti-inflammatory formulations. Future investigations, including *in vivo* studies and toxicity profiling, are essential to validate their clinical relevance and safety for biomedical use.

ACKNOWLEDGEMENTS

The authors are thankful to the Principal and Faculty of MVP's College of Pharmacy for providing the essential research facilities and support to conduct the study.

CONFLICT OF INTEREST

The authors declare that there is no conflict of interests regarding the publication of this article.

REFERENCES

1. M.F. Al-Hakkani, *SN Appl. Sci.*, **2**, 505 (2020); https://doi.org/10.1007/s42452-020-2279-1
2. S.A. Akintelu, A.S. Folorunso, F.A. Folorunso and A.K. Oyebamiji, *Heliyon*, **6**, e04508 (2020); https://doi.org/10.1016/j.heliyon.2020.e04508
3. M. Thatyana, N.P. Dube, D. Kemboi, A.L.E. Manicum, N.S. Mokgalaka-Fleischmann and J.V. Tembu, *Nanomaterials*, **13**, 2616 (2023); https://doi.org/10.3390/nano13192616
4. R. Prakruthia and H.N. Deepakumari, *RSC Adv.*, **14**, 28703 (2024); https://doi.org/10.1039/D4RA04622F
5. A. Jayadev and B.N. Krishnan, *J. Sci. Res.*, **65**, 80 (2021); https://doi.org/10.37398/JSR.2021.650111
6. H. Gebrehiwot, A. Dekebo, K. Shenkute, U. Ensermu and M. Endale, *Bull. Chem. Soc. Ethiop.*, **38**, 167 (2023); https://doi.org/10.4314/bcse.v38i1.13
7. K. Mendam and S.J.K. Naik, *Mater. Today: Proc.*, **92**, 618 (2023); https://doi.org/10.1016/j.matpr.2023.04.126
8. A.A. Wakchaure, M.R. Kumbhare, G.B. Jadhav, S.R. Gawali and K.N. Mundlod, *Res. J. Pharm. Technol.*, **18**, 4047 (2025); https://doi.org/10.52711/0974-360X.2025.00581
9. O.A. Olalere and C.Y. Gan, *Sep. Sci. Technol.*, **56**, 1853 (2021); https://doi.org/10.1080/01496395.2020.1795678
10. M. Ramzan, R.M. Obodo, S. Mukhtar, S.Z. Ilyas, F. Aziz and N. Thovhogi, *Mater. Today Proc.*, **36**, 576 (2021); https://doi.org/10.1016/j.matpr.2020.05.472
11. S.D. Bhinge, M.G. Hogade, A.S. Savali, H.R. Chitapurkar and C.S. Magdum, *Indian Drugs*, **50**, 44 (2013); https://doi.org/10.53879/id.50.05.p0044
12. M. Balouiri, M. Sadiki and S.K. Ibnsouda, *J. Pharm. Anal.*, **6**, 71 (2016); https://doi.org/10.1016/j.jpha.2015.11.005
13. P. Siva Krishna, P. Srinivasa Babu and R. Karthikeyan, *CIBTech J. Pharm. Sci.*, **6**, 19 (2017).
14. A. Chowdhury, S. Azam, M.A. Jainul, K.O. Faruq and A. Islam, *Int. J. Microbiol.*, **2014**, 410935 (2014); https://doi.org/10.1155/2014/410935
15. C.A. Winter, E.A. Risley and G.W. Nuss, *Exp. Biol. Med.*, **111**, 544 (1962); https://doi.org/10.3181/00379727-111-27849
16. P. Belle, E. Kedi, A.A. Ntoumba and B. Moll, *Int. J. Green Herb. Chem.*, **9**, (2020); https://doi.org/10.24214/IJGHC/HC/9/3/34560
17. P. Belle, E. Kedi, F. Eya'ane Meva, L. Kotsedi, E.L. Nguemfo, C. Bogning Zangueu, A.A. Ntoumba, H. Mohamed, A.B. Dongmo and M. Maaza, *Int. J. Nanomedicine*, **13**, 8537 (2018); https://doi.org/10.2147/IJN.S174530
18. B. Sadeghi and F. Gholamhoseinpoor, *Spectrochim. Acta A Mol. Biomol. Spectrosc.*, **134**, 310 (2015); https://doi.org/10.1016/j.saa.2014.06.046
19. E.A. Mohamed, *Heliyon*, **6**, e03123 (2020); https://doi.org/10.1016/j.heliyon.2019.e03123
20. K. Velsankar, R.M. Aswin Kumara, R. Preethi, V. Muthulakshmi and S. Sudhahar, *J. Environ. Chem. Eng.*, **8**, 104123 (2020); https://doi.org/10.1016/j.jece.2020.104123
21. G. Madec, P. Delecluse, M. Imbard and C. Levy, OPA 8.1 Ocean General Circulation Model Reference Manual. Notes du Pôle Modélisation, Inst Pierre Simon Laplace (1998)
22. Y.S. Hajizadeh, N. Harzandi, E. Babapour, M. Yazdanian and R. Ranjbar, *Adv. Mater. Sci. Eng.*, **2022**, 8100440 (2022); https://doi.org/10.1155/2022/8100440
23. V.U. Siddiqui, A. Ansari, R. Chauhan and W.A. Siddiqi, *Mater. Today Proc.*, **36**, 751 (2021); https://doi.org/10.1016/j.matpr.2020.05.504
24. M.T. Shaaban, M.F. Ghaly and S.M. Fahmi, *J. Basic Microbiol.*, **61**, 557 (2021); https://doi.org/10.1002/jobm.202100061